Cosmological Constraints on the Phenomenological Interacting Dark Energy Model with *Fermi* Gamma-Ray Bursts and DESI DR2

Ziyan Zhu^{a,1}, Qingquan Jiang^{b,2}, Yu Liu^{c,3}, Puxun Wu^{d,4}, Nan Liang^{a,*}

Abstract

In this work, we constrain the phenomenological interacting dark energy (IDE) model using Fermi gamma-ray burst (GRB) dataset and the latest baryon acoustic oscillation (BAO) data from the Dark Energy Spectroscopic Instrument (DESI) Data Release 2 (DR2). Through a joint Bayesian analysis, we perform a cosmological comparative assessment of the Λ CDM, wCDM, and CPL models with the phenomenological IDE model. For the phenomenological IDE model in a flat universe, we obtain: $\xi = 2.644^{+1.144}_{-0.933}$, $\xi + 3w_X = -1.001^{+2.827}_{-3.153}$ with the GOLD sample ($z \geq 1.4$) and DESI DR2; and $\xi = 2.879^{+0.995}_{-0.990}$, $\xi + 3w_X = 0.086^{+1.365}_{-1.440}$ with the FULL sample ($z \geq 1.4$) and DESI DR2. Our analysis shows that the Λ CDM model without interaction are consistent with the latest Fermi sample and DESI DR2 at 1σ confidence level.

Keywords: gamma-ray bursts: general - (cosmology:) dark energy - cosmology: observations

1. INTRODUCTION

The discovery of the universe's accelerated expansion via Type Ia supernovae (Riess et al., 1998; Perlmutter et al., 1999) cemented the Λ CDM model as the standard cosmological paradigm, which is plagued by fundamental theoretical puzzles, including the fine-tuning and coincidence problems (Weinberg, 1989; Carroll, 2001). Moreover, increasingly precise observations have revealed the Hubble tension (Di Valentino et al., 2025): a $\gtrsim 5\sigma$ discrepancy of H_0 between the locally measured value (Riess et al., 2022) and the value inferred from the Cosmic Microwave Background (CMB) under the Λ CDM assumption (Planck Collaboration, 2020), which may point to new physics beyond the standard model. These challenges motivate the exploration of dynamical dark energy (DE) models and extensions to the standard model (Copeland et al., 2006; Li et al., 2011). The Chevallier-Polarski-Linder (CPL) parameterization (Chevallier & Polarski, 2001; Linder, 2003) provides a widely used framework for testing time-varying dark energy through the equation of state (EoS) $w(z) = w_0 + w_a z/(1+z)$, where w_0 represents the present value and w_a characterizes its time evolution.

^{*}Corresponding author: liangn@bnu.edu.cn

¹zzy@gznu.edu.cn

²qqjiangphys@yeah.net

³lyu@swjtu.edu.cn

⁴pxwu@hunnu.edu.cn

The interacting dark energy (IDE) models, which allow for a direct energy-momentum exchange between dark energy and dark matter (DM), have garnered significant attention to alleviate the coincidence problem. (Amendola, 2000; Zimdahl et al., 2001; Wang et al., 2019; Yang et al., 2021; Costa et al., 2019) Moreover, the interaction between DE and DM can modify the background expansion history and the growth of structure, leading to an increased value of H_0 . Therefore, the IDE models can potentially reconcile observational discrepancies to alleviate the Hubble tension (Pan et al., 2019, 2020; Kumar & Nunes, 2019; Di Valentino et al., 2021; Abdalla et al., 2022).

The phenomenological scenario can be explored the IDE model by considering the ratio of the energy densities of dark energy to matter as (Dalal et al., 2001) $r \equiv \rho_X \propto \rho_m a^\xi$, where ρ_X and ρ_m are the energy densities of dark energy and matter, respectively. The cases where $\xi=3$ and $\xi=0$ correspond to the Λ CDM model and a self-similar solution without the coincidence problem, respectively; values of $0 \le \xi \le 3$ indicate a less severe coincidence problem. In a flat FRW (Friedmann-Robertson-Walker) universe, the interaction term can be obtained by $Q=-H\rho_m(\xi+3w_X)$, where w_X represents the EoS for DE. The condition $\xi+3w_X\neq 0$ denotes the interacting scenario. Some early studies investigated the phenomenological model with the joint data utilizing SNe Ia, CMB, as well as the baryon acoustic oscillations (BAOs) and the observational Hubble data (OHD), which indicated that the coincidence problem was not alleviated (Guo et al., 2007; Chen et al., 2010; Cao, Liang & Zhu, 2011). However, many works found that the latest data suggest energy transfer from DE to DM (Wang, 2022; Goswami and Das, 2025). Moreover, it is interesting to find that the energy flow transfer between DE and DM with sign shifting interaction functions Halder et al. (2024) and Li et al. (2026).

The observational data in the redshift region between the local distance ladder calibrated by Cepheids (z < 0.01) and CMB ($z \sim 1000$) might offer important insights into the origins of the H_0 tension. Other observational data have also been used to constrain the phenomenological IDE models, e.g., strong gravitational lensing (SGL) data (Cheng et al., 2021), mock data of gravitational waves (GWs) (Zheng et al., 2022; Hou et al., 2023; Li et al., 2024a), as well as the mock and localized Fast radio bursts (FRBs) (Zhao et al., 2023; Yan et al., 2025). The Dark Energy Spectroscopic Instrument (DESI) release the BAO data DR1 (DESI Collaboration, 2024) to suggest that dark energy may not be a cosmological constant with new insights (Colgáin et al., 2026). Li et al. (2024b, 2025) utilize the DESI DR1 in combination with the SN data and the CMB data to explore potential interactions between DE and DM.

Gamma-ray bursts (GRBs) are the most intense explosions observed to reach a higher maximum observable redshift at $z \sim 10$ (Cucchiara et al., 2011). The luminosity relations of GRBs with known redshift between measurable spectroscopic properties and their luminosity or energy have been proposed to investigate cosmology (Amati et al., 2002; Ghirlanda et al., 2004; Yonetoku et al., 2004; Dai et al., 2004; Schaefer, 2007). In order to avoid the circularity problem, Liang et al. (2008) introduced a cosmological model-independent method for calibrating the luminosity relations of GRBs by utilizing data from SNe Ia. On the other hand, Amati et al. (2008) also proposed the simultaneous fitting method which constrain the coefficients of the relationship and the parameters of the cosmological model simultaneously. Furthermore, Amati et al. (2019) proposed an alternative approach for calibrating the Amati relation of 193 GRBs using OHD obtained from the cosmic chronometers (CC) method by simultaneous fitting with the Bézier parametric. Therefore, GRBs data can be employed to place constraints on cosmological models without the circularity problem (Liang et al., 2008, 2010, 2011, 2022; Kodama et al., 2008; Wei, 2010; Wang et al., 2016a; Demianski et al., 2017; Wang et al., 2019; Amati et al., 2008, 2019; Luongo & Muccino, 2021; Liu et al., 2022; Li et al., 2023; Cao & Ratra, 2024; Alfano et al., 2025; Huang et al., 2025; Bargiacchi et al., 2025).

Recently, Khadka et al. (2021) made a compilation with the Amati relation (Amati et al., 2002) comprising 118 GRBs (A118) with the smallest intrinsic dispersion from a broader set of 220 GRBs (A220). Liang et al. (2022) calibrated the A219 sample ⁵ from the Pantheon sample (Scolnic et al., 2018) by using a Gaussian Process to constrain DE models with GRBs at high redshift. Wang et al. (2024) investigate the phenomenologically emergent dark energy (PEDE) model with A118 sample and OHD at intermediate redshift.

More recently, Nong & Liang (2024) tested the phenomenological IDE model with Pantheon+ SNe Ia and A118 GRB dataset. Wang & Liang (2024) presented a sample of long GRBs from 15 years of the *Fermi*-GBM (Gamma-ray Burst Monitor) catalogue with identified redshift, in which the GOLD sample contains 123 long GRBs at $z \leq 5.6$ and the FULL sample contains 151 long GRBs with redshifts at $z \leq 8.2$. Cao & Ratra (2025) analyzed the *Fermi*-observed long GRBs datasets (Wang & Liang, 2024) to simultaneously constrain the Amati correlation and cosmological parameters within six spatially flat and nonflat DE models.

The latest measurements from DESI DR2 (DESI Collaboration, 2025) provided exquisite distance constraints at intermediate redshifts (0.3 < z < 2.3). In this paper, we investigate the specific phenomenological IDE model with the updated sample from the *Fermi* satellite (Wang & Liang, 2024) and the latest baryon acoustic oscillation measurements from DESI DR2 (DESI Collaboration, 2025). This approach allows us to place robust constraints on the interaction strength ξ and the dark energy equation-of-state parameter w_X , as well as to test the time evolution of dark energy through the CPL parameterization, thereby extending the cosmological probe to higher redshifts and breaking parameter degeneracies among different dark energy models.

2. PHENOMENOLOGICAL INTERACTING DARK ENERGY MODEL

The phenomenological interacting dark energy model serves as a useful parameterization for several theoretically motivated scenarios, which introduces a coupling term Q in the continuity equations, ensuring total energy-momentum conservation (Amendola, 2000)

$$\dot{\rho}_m + 3H\rho_m = Q,\tag{1}$$

$$\dot{\rho}_X + 3H(1+w_X)\rho_X = -Q,\tag{2}$$

where ρ_m and ρ_X are the energy densities of dark matter and dark energy, respectively, w_X is the dark energy equation-of-state parameter, $H \equiv \dot{a}/a$ is the Hubble parameter, and overdots denote derivatives with respect to cosmic time. The sign convention for Q follows: Q > 0 implies energy transfer from dark energy to dark matter.

In this work, we use ξ IDE to represent the phenomenological interaction model (Dalal et al., 2001), with the energy density ratio defined as:

$$\frac{\rho_X}{\rho_m} \propto a^{\xi},\tag{3}$$

where ξ quantifies the interaction strength. This ansatz leads to the interaction function:

$$Q = -H\rho_m(\xi + 3w_X)\Omega_X,\tag{4}$$

where $\Omega_X \equiv \rho_X/(\rho_m + \rho_X)$ is the DE density fraction. The sign of the combination $(\xi + 3w_X)$ dictates the direction of energy flow: negative values of $(\xi + 3w_X)$ corresponds to Q > 0 with a transfer of energy from DE to DM.

⁵Removed GRB051109A, which are counted twice in the A220 sample (Khadka et al., 2021).

The background evolution is governed by the Friedmann equation:

$$H^{2} = \frac{8\pi G}{3}(\rho_{m} + \rho_{X}),\tag{5}$$

with the explicit solution for the Hubble parameter in a flat FRW universe:

$$H(z) = H_0 \left[(1 - \Omega_{m0})(1+z)^{3(1+w_X)+\xi} + \Omega_{m0}(1+z)^3 \right]^{1/2} \times \left[\frac{\Omega_{m0} + (1 - \Omega_{m0})(1+z)^{-\xi}}{1 + (1 - \Omega_{m0})/\Omega_{m0}} \right]^{-3w_X/(2\xi)}.$$
(6)

3. DATA AND METHODOLOGY

In this work, we employ the updated sample of GRBs from the *Fermi* satellite (Wang & Liang, 2024), in which the GOLD sample contains 123 data at $z \leq 5.6$ and the FULL sample contains 151 data with redshifts at $z \leq 8.2$. the latest BAO measurements from the second data release (DR2) of the DESI (DESI Collaboration, 2025), which provide precise measurements across a redshift range of 0.3 < z < 2.3. The Amati relation (Amati et al., 2002), which correlates the spectral peak energy $E_{\rm p,i}$ and the isotropic-equivalent radiated energy $E_{\rm iso}$:

$$\log_{10}\left(\frac{E_{\rm iso}}{1 \text{ erg}}\right) = a + b\log_{10}\left(\frac{E_{\rm p,i}}{300 \text{ keV}}\right). \tag{7}$$

The Fermi-GBM catalogue at low-redshift can be calibrated from the latest OHD with the cosmic chronometers method by using a Gaussian Process to obtained GRBs at high-redshift $z \geq 1.4$. The corresponding χ^2 function is defined as:

$$\chi_{\text{GRB}}^2 = \sum_{i=1}^{N_{\text{GRB}}} \frac{[\mu_{\text{obs}}(z_i) - \mu_{\text{th}}(z_i; \mathbf{p}, H_0)]^2}{\sigma_{\mu, i}^2},$$
(8)

where μ_{obs} and μ_{th} are the observed and theoretical distance moduli, and **p** represents the cosmological parameters, N_{GRB} represents the Number of *Fermi* GRBs at $z \geq 1.4$: for the GOLD sample, $N_{\text{GRB}} = 60$; and for the FULL sample, $N_{\text{GRB}} = 78$, respectively. The BAO observable is expressed as:

$$\chi_{\text{BAO}}^2 = (\mathbf{D}_{\text{obs}} - \mathbf{D}_{\text{th}})^T \mathbf{C}_{\text{BAO}}^{-1} (\mathbf{D}_{\text{obs}} - \mathbf{D}_{\text{th}}), \tag{9}$$

where $\mathbf{D} = [D_M(z)/r_d, H(z)r_d]$, $D_M(z)$ is the comoving angular diameter distance, H(z) is the Hubble parameter, and r_d is the sound horizon at the drag epoch.⁶ We utilize the full covariance matrix from DESI DR2⁷, which includes correlations between different redshift bins and between $D_M(z)/r_d$ and $H(z)r_d$ measurements.

$$r_d = \int_{z_d}^{\infty} \frac{c_s(z)}{H(z)} dz, \tag{10}$$

where z_d is the redshift at the drag epoch and $c_s(z)$ is the sound speed in the baryon-photon fluid. The sound horizon r_d is treated as a free parameter derived consistently within each cosmological model, ensuring self-consistent comparison of the BAO scale across different cosmological models (Beutler et al., 2011)

⁶The sound horizon r_d is computed self-consistently for each cosmological model by integrating the sound speed in the baryon-photon fluid over the modified expansion history H(z):

⁷https://github.com/CobayaSampler/bao_data/tree/master/desi_bao_dr2

The total likelihood combines baryon acoustic oscillation and gamma-ray burst datasets:

$$\mathcal{L}_{\text{total}} = \mathcal{L}_{\text{BAO}} \times \mathcal{L}_{\text{GRB}},$$
 (11)

with the corresponding χ^2 function:

$$\chi_{\text{total}}^2 = \chi_{\text{GRB}}^2 + \chi_{\text{BAO}}^2. \tag{12}$$

Our cosmological analysis encompasses four DE models:

- Λ CDM: The standard cosmological model with Ω_m and H_0 as free parameters;
- wCDM: Extension with constant dark energy equation of state w as an additional parameter;
- CPL: Dynamical dark energy with time-varying equation of state $w(z) = w_0 + w_a z/(1+z)$;
- ξ **IDE:** Interacting dark energy with coupling parameter ξ and equation of state w_X .

For the Markov Chain Monte Carlo analysis, we employ the **emcee** Python package (Foreman-Mackey et al., 2013). Parameter inference and uncertainty quantification are performed using its affine-invariant ensemble sampler. Posterior distributions obtained from both configurations are in excellent agreement, demonstrating the stability of the sampling and the reliability of our results. Throughout the analysis, all cosmological parameters are assigned physically motivated priors.

4. RESULTS

The joint analysis of DESI DR2 measurements and Fermi GRBs provides tight constraints on cosmological parameters while allowing for robust model discrimination. Figure 1 shows comparative constraints from the GOLD and FULL sample at $z \ge 1.4$) for different cosmological models, facilitating direct comparison between the GOLD and FULL samples at high redshifts ($z \ge 1.4$). We summarize results of the four DE models with parameter constraints and model selection statistics in Table 1.

Table 1: Comparative cosmological constraints at 1σ confidence level from the GOLD and FULL sample at $z \ge 1.4$ combined with DESI BAO measurements.

Dataset	Model	H_0	Ω_m	w/w_0	w_X/w_a	ξ	$-2 \ln \mathcal{L}_{\max}$	$\Delta { m AIC}$	$\Delta \mathrm{BIC}$
GOLD+BAO	$\Lambda \mathrm{CDM}$	68.93 ± 0.64	$0.298^{+0.025}_{-0.023}$	-	-	-	205.400	0.000	0.000
	wCDM	$67.98^{+1.68}_{-1.41}$	$0.294^{+0.026}_{-0.026}$	$-0.937^{+0.204}_{-0.238}$	-	_	210.422	7.022	12.000
	CPL	$68.2^{+2.1}_{-1.8}$	$0.296^{+0.050}_{-0.075}$	$-1.133^{+2.007}_{-1.762}$	$0.116^{+1.002}_{-1.101}$	-	216.520	15.120	28.470
	$\xi \mathrm{IDE}$	67.8 ± 1.5	$0.392^{+0.246}_{-0.291}$	-	$-1.215^{+0.629}_{-0.740}$	$2.644^{+1.144}_{-0.933}$	214.365	12.965	36.510
FULL+BAO	$\Lambda \mathrm{CDM}$	68.91 ± 0.63	$0.298^{+0.024}_{-0.022}$	-	-	-	205.436	0.000	0.000
	wCDM	$67.95^{+1.65}_{-1.43}$	$0.294^{+0.026}_{-0.027}$	$-0.942^{+0.221}_{-0.222}$	-	_	210.422	6.986	15.360
	CPL	$68.3^{+2.0}_{-1.7}$	$0.292^{+0.053}_{-0.083}$	$-1.026^{+1.919}_{-1.876}$	$0.060^{+1.067}_{-1.075}$	-	216.407	14.971	38.630
	$\xi \mathrm{IDE}$	67.7 ± 1.6	$0.286^{+0.208}_{-0.202}$	-	$-0.931^{+0.366}_{-0.480}$	$2.879_{-0.990}^{+0.995}$	214.720	13.284	30.030

Note. \triangle AIC and \triangle BIC are calculated relative to the \triangle CDM model for each dataset.

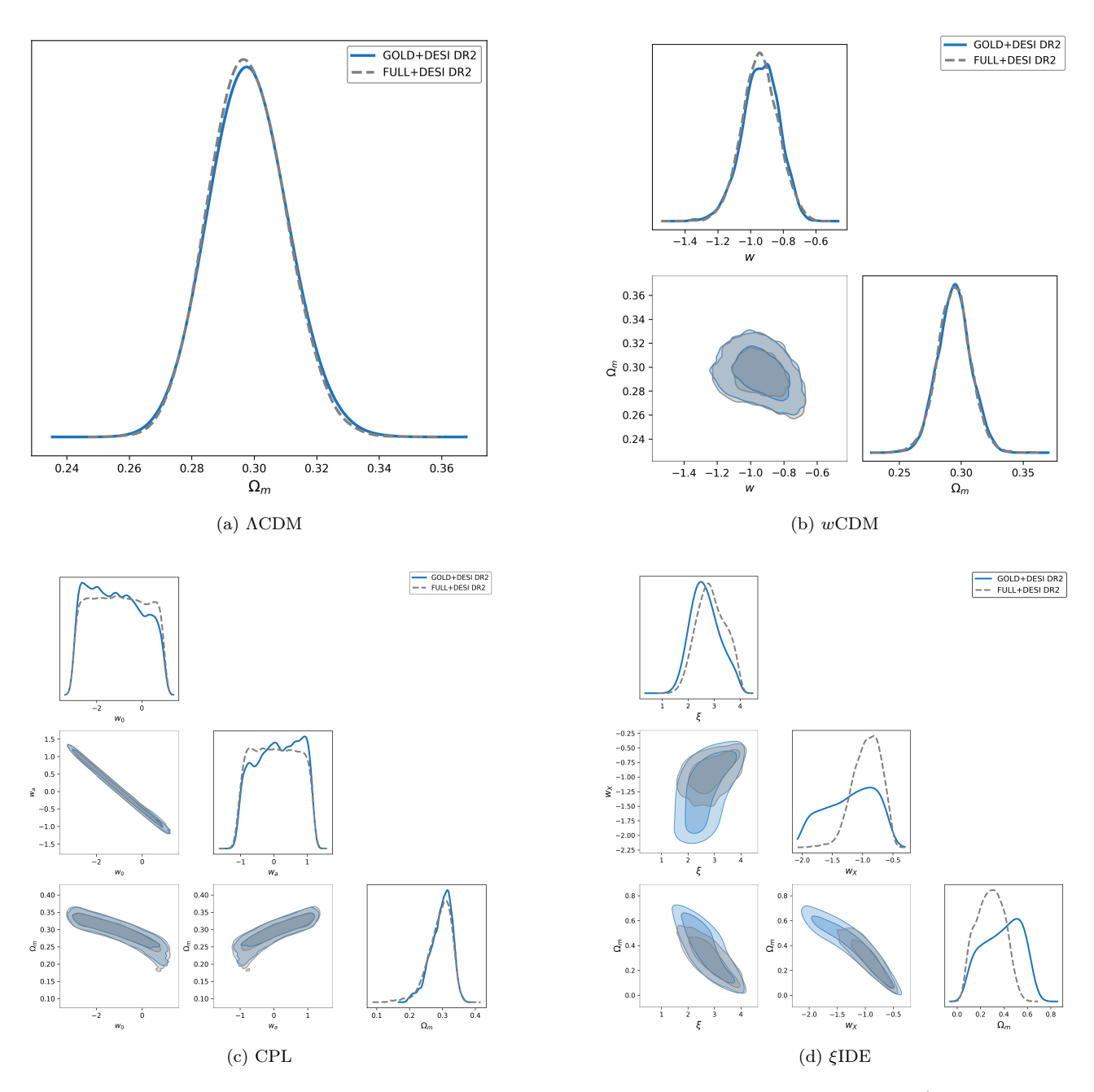


Figure 1: Comparative constraints on cosmological parameters from the GOLD GRB dataset (blue, 60 GRBs at $z \ge 1.4$) and FULL GRB dataset (gray, 78 GRBs at $z \ge 1.4$) for different cosmological models: (a) Λ CDM model; (b) wCDM model; (c) CPL model; (d) ξ IDE model.

From Figure 1 and Table 1, we find that the results with GOLD and FULL sample are consistent within 1σ uncertainties. For the Λ CDM model, the results from the two GRB samples are fully consistent and in excellent agreement with Planck CMB measurements (Planck Collaboration, 2020). For the wCDM model, the constraints obtained from both samples are consistent with the cosmological constant value (w = -1) at the 1σ confidence level. For the CPL model, the values of w_a are consistent with zero within its 1σ uncertainty, which suggest that current data cannot support the time evolution of the DE EoS. For the ξ IDE model, the energy flow parameter ($\xi + 3w_X$) with both samples shows sample dependence and remains consistent with no energy exchange within 1σ uncertainties, indicating no statistically significant preference for any particular transfer direction (Cai & Wang, 2010; Clemson et al., 2012; Borges & Carneiro, 2008). The combined analysis of high-redshift GRB data and DESI DR2 BAO measurements shows a consistent preference for the Λ CDM framework.

Finally, we compare these DE models with Akaike Information Criterion (AIC), Bayesian Information Criterion (BIC). The Δ AIC and Δ BIC values of the four cosmological models with the Λ CDM model as the reference indicate that the the wCDM, CPL and ξ IDE models have essentially no empirical support compared to the Λ CDM model. The estimated parameters of three extended models remain consistent with the expectations of Λ CDM within 1σ uncertainties.

Constraints on the parameters of the ξ IDE models compared with previous studies (Guo et al., 2007; Chen et al., 2010; Cao, Liang & Zhu, 2011; Salvatelli et al., 2014; Wang et al., 2016b; Yang et al., 2021; Zheng et al., 2022; Nong & Liang, 2024) tested the phenomenological IDE model with A118 GRB sample and Pantheon+ SNe Ia dataset, a joint sample of SNe, BAO, and CMB data, and a combination of CMB, BAO, and Redshift Space Distortion (RSD) data, as well as the Supernova Legacy Survey (SNLS) and the mock GW data, which are summarised Table 2. Compared to the results in the early studies (Guo et al., 2007; Chen et al., 2010; Cao, Liang & Zhu, 2011; Zheng et al., 2022): $\xi > 3$, which indicated that the coincidence problem was not alleviated, and ξ close to 0 which correspond to a self-similar solution without the coincidence problem (Salvatelli et al., 2014; Wang et al., 2016b; Yang et al., 2021); our analysis with high-redshift GRBs and DESI DR2 find the values of $\xi < 3$, which indicate that the coincidence problem can be alleviated; as well as the values of ξ close to 3 and $(\xi + 3w_X)$ to 0, which are consistent with the Λ CDM model without interaction.

Table 2: Comparison of constraints for the IDE models at 1σ confidence level from different studies.

Study	Dataset	ξ	w_X	$\xi + 3w_X$	
This work	$_{\mathrm{GOLD+BAO}}$	$2.64_{-0.93}^{+1.14}$	$-1.22^{+0.63}_{-0.74}$	$-1.00^{+2.83}_{-3.15}$	
	$_{\rm FULL+BAO}$	$2.88^{+1.00}_{-0.99}$	$-0.93^{+0.37}_{-0.48}$	$0.09^{+1.37}_{-1.44}$	
Nong & Liang (2024)	A118 + Pantheon +	0.54 ± 0.36	$-1.02^{+0.16}_{-0.18}$	-2.52 ± 0.87	
Zheng et al. (2022)	GW (Mock)	$3.05^{+0.77}_{-0.45}$	$-1.24^{+0.38}_{-0.41}$	$-0.67^{+1.79}_{-1.58}$	
Yang et al. (2021)	$_{\rm CMB+BAO+RSD}$	0.08 ± 0.07	-1.02 ± 0.03	-2.98 ± 0.08	
Wang et al. (2016b)	$_{\mathrm{CMB+BAO+SN}}$	0.20 ± 0.30	-1.10 ± 0.10	-3.10 ± 0.40	
Salvatelli et al. (2014)	$CMB+SN+H_0$	$-0.60^{+0.12}_{-0.13}$	-0.98 ± 0.02	$-3.54^{+0.12}_{-0.13}$	
Cao, Liang & Zhu (2011)	$H(z)+{ m BAO}+{ m CMB}$	$3.35^{+1.37}_{-1.32}$	$-1.11^{+0.38}_{-0.43}$	$-0.02^{+2.35}_{-2.38}$	
Chen et al. (2010)	SNe+BAO+CMB	3.06 ± 0.35	-0.98 ± 0.07	0.12 ± 0.56	
Guo et al. (2007)	SNLS+BAO+CMB	$3.36^{+0.69}_{-0.70} (2\sigma)$	$-1.03^{+0.12}_{-0.15} (2\sigma)$	$-0.20^{+0.34}_{-0.35} (2\sigma)$	

Note. In this work, our results show two constraints using GOLD (60 GRBs) and FULL (78 GRBs) samples at $z \ge 1.4$ with DESI DR2.

5. CONCLUSION AND DISCUSSIONS

In this work, we constrain the phenomenological IDE model using Fermi GRB dataset with the Amati relation and the latest BAO data from DESI DR2. Our comprehensive analysis with the ξ IDE model shows statistically significant non-zero interaction strength in both samples ($\xi = 2.644^{+1.144}_{-0.933}, \xi + 3w_X = -1.001^{+2.827}_{-3.153}$ for GOLD and $\xi = 2.879^{+0.995}_{-0.990}, \xi + 3w_X = 0.086^{+1.365}_{-1.440}$ for FULL), which are consistent with the Λ CDM model without energy exchange ($\xi + 3w_X = 0$) within 1σ uncertainties. For the CPL parameterization, which shows large uncertainties in the dark energy evolution parameters, we find w_a consistent with zero at 1σ confidence level, indicating no evidence for time-varying dark energy equation of state. The Δ AIC and Δ BIC values indicate that the the wCDM, CPL and ξ IDE models have essentially no empirical support compared to the Λ CDM model. However, none of the considered models significantly alleviates the Hubble tension, with all yielding H_0 values consistent with early-universe measurements.

The decisive statistical preference for wCDM over the CPL and ξ IDE model indicates that current data do not require exotic dark sector interactions or time-varying dark energy beyond a simple $w \neq -1$ dark energy. However, our analysis considers only one specific phenomenological coupling form and a particular parameterization for dynamical dark energy; other theoretically motivated interaction functions and dark energy parameterizations may yield different conclusions. The cosmological constraints at high-redshift come primarily from GRBs, which are sensitive to dark sector interactions with larger systematic uncertainties than low-redshift probes, are not included in our purely geometric analysis.

In conclusion, both the IDE scenario and dynamical DE models remain theoretically motivated and observationally testable frameworks that warrant continued investigation with future precision datasets, which will dramatically improve cosmological constraints by providing better-calibrated GRB samples. The French-Chinese satellite spacebased multi-band astronomical variable objects monitor (SVOM) will allow for a more stringent test of the phenomenological framework.

Declaration of competing interest

The authors declare that they have no known competing financial interests or personal relationships that could have appeared to influence the work reported in this paper.

ACKNOWLEDGMENTS

This project was supported by the Guizhou Provincial Science and Technology Foundation: QKHJC-ZK[2021] Key 020 and QKHJC-ZK[2024] general 443. Q. Jiang was supported by the Sichuan Provincial Key Projects for Science-Education Integration (25LHJJ0097). Y. Liu was supported by the NSFC under Grant No. 12373063. P. Wu was supported by the National Natural Science Foundation of China (Grant No. 12275080).

DATA AVAILABILITY

Data are available at the following references: the DESI DR2 BAO data from DESI Collaboration (2025), the *Fermi* gamma-ray burst sample from Wang & Liang (2024).

References

Abdalla E. et al., 2022, JHEAP, 34, 49

Alfano, A., Luongo, O., Muccino, M. 2025, JHEAP, 46, 100348

Amati L. et al., 2002, A&A, 390, 81

Amati L. et al., 2008, MNRAS, 391, 577

Amati L., D'Agostino R., Luongo O. et al., 2019, MNRAS, 486, L46

Amendola L., 2000, Phys. Rev. D, 62, 043511

Bargiacchi, G., Dainotti, M. G., & Hernandez, X. 2025, New Astronomy Reviews, 100, 101712

Beutler F. et al., 2011, MNRAS, 416, 3017

Borges H. A., Carneiro S., 2008, Gen. Relativ. Gravit., 40, 1893

Brout D. et al., 2022, ApJ, 938, 110

Cai R.-G., Wang A., 2010, JCAP, 03, 002

Cao S., Liang N., Zhu Z.-H., 2011, MNRAS, 416, 1099

Cao, S. & Ratra, B. 2024, JCAP, 10, 093

Cao S., & Ratra, B., 2025, JCAP, 09, 081

Carroll S. M., 2001, Living Rev. Relativ., 4, 1

Chevallier M., Polarski D., 2001, Int. J. Mod. Phys. D, 10, 213

Chen Y., Zhu Z.-H., Alcaniz J. S., Gong Y., 2010, ApJ, 711, 439

Cheng W., He Y., Diao J.-W., Pan Y., Zeng J., Zhang J.-W., 2021, JHEP, 08, 124

Clemson T. et al., 2012, Phys. Rev. D, 85, 043007

Colgáin, E. O., Dainotti, M. G., Capozziello, S., et al., 2026, JHEAP, 49, 100428

Copeland E. J., Sami M., Tsujikawa S., 2006, Int. J. Mod. Phys. D, 15, 1753

Costa A. A., Xu X.-D., Wang B., Ferreira E. G. M., 2019, Phys. Rev. D, 89, 103531

Cucchiara A., Levan A. J., Fox D. B. et al., 2011, ApJ, 736, 7

Dai Z. G., Liang E. W., Xu D., 2004, ApJ, 612, L101

Dalal N., Abazajian K., Jenkins E., Manohar A. V., 2001, Phys. Rev. Lett., 87, 141302

Di Valentino, E. Said, J. L., Riess, A. et al., 2025, Physics of the Dark Universe, 49, 101965

Demianski M., Piedipalumbo E., Sawant D., Amati L., 2017, A&A, 598, A112

DESI Collaboration, 2024, arXiv:2404.03000

DESI Collaboration et al., 2025, arXiv:2503.14738v2 [astro-ph.CO]

Di Valentino E. et al., 2021, Astropart. Phys., 131, 102604

Foreman-Mackey D. et al., 2013, PASP, 125, 306

Goswami S. and Das S., 2025, Physics of the Dark Universe, 48, 101951

Ghirlanda G., Ghisellini G., Lazzati D., 2004, ApJ, 616, 331

Guo, Z.-K., Ohta, N., & Tsujikawa, S. 2007, Phys. Rev. D, 76, 023508

Halder, S., de Haro, J., Saha, T., & Pan, S. 2024, arXiv:2403.01397 [gr-qc]

Hou W. T., Qi J. Z., Han T. et al., 2023, JCAP, 05, 017

Huang, Z., Xiong, Z., Luo, X., Wang, G., Liu, Y., Liang, N. 2025, JHEAP, 47, 100337

Khadka N., Luongo O., Muccino M., Ratra B., 2021, JCAP, 09, 042

Kodama Y., Yonetoku D., Murakami T., 2008, MNRAS, 391, L1

Kumar S., Nunes R. C., 2019, Phys. Rev. D, 96, 103511

Li M., Li X.-D., Wang S., Wang Y., 2011, JCAP, 09, 021

Li Z. H., Zhang B., Liang N., 2023, MNRAS, 521, 4406

Li T.-N., Jin S.-J., Li H.-L., Zhang J.-F., Zhang X., 2024, ApJ, 963, 52

Li T.-N., Wu P.-J., Du G.-H., Jin S.-J., Li H.-L., Zhang J.-F., Zhang X., 2024, ApJ, 976, 1

Li T.-N., Du G.-H., Li Y.-H. et al., 2025, Eur. Phys. J. C, 85, 608

Li T.-N., Du G.-H., Li Y.-H. Wu P.-J., Jin S.-J., Zhang J.-F., Zhang X., 2026, Sci. China-Phys. Mech. Astron. 69, 210413

Liang N., Xiao W. K., Liu Y., Zhang S. N., 2008, ApJ, 685, 354

Liang N., Wu P. X., Zhang S. N., 2010, Phys. Rev. D, 81, 083518

Liang N., Xu L., Zhu Z. H., 2011, A&A, 527, A11

Liang N., Li Z., Xie X., Wu P., 2022, ApJ, 941, 84

Linder E. V., 2003, Phys. Rev. Lett., 90, 091301

Liu, Y., Liang, N., Xie, X., et al. 2022, ApJ, 935, 7

Luongo, O., & Muccino, M. 2021, MNRAS, 503, 4581

Nong X.-D., Liang N., 2024, RAA, 24, 12, 125003

Pan S., Yang W., Di Valentino E., Saridakis E. N., Chakraborty S., 2019, Phys. Rev. D, 100, 103520

Pan S., Yang W., Paliathanasis A., 2020, MNRAS, 493, 3114

Perlmutter S. et al., 1999, ApJ, 517, 565

Planck Collaboration, 2020, A&A, 641, A6

Riess A. G. et al., 1998, AJ, 116, 1009

Riess A. G. et al., 2022, ApJ, 938, 36

Salvatelli V., Said N., Bruni M. et al., 2014, Phys. Rev. Lett., 113, 181301

Schaefer B. E., 2007, ApJ, 660, 16

Scolnic D. M., Jones D. O., Rest A. et al., 2018, ApJ, 859, 101

Wang, J. S., Wang, F. Y., Cheng, K. S., & Dai, Z. G. 2016, A&A, 585, A68

Wang B., Abdalla E., Atrio-Barandela F., Pavón D., 2016, JCAP, 01, 052

Wang, Y. Y., & Wang, F. Y. 2019, ApJ, 873, 39

Wang B. et al., 2019, MNRAS, 487, 882

Wang H., Liang N., 2024, MNRAS, 533, 743

Wang, G., Li, X., & Liang, N. 2024, ApSS, 369, 74

Wang, D. 2022, Phys. Rev. D, 106, 063515

Wei H., 2010, JCAP, 08, 020

Weinberg S., 1989, Rev. Mod. Phys., 61, 1

Yan H., Pan Y., Wang J.-X., Xu W.-X., Peng Z.-H. 2025, Chinese Physics C, 49, 11, 115109

Yang W. et al., 2021, JCAP, 10, 032

Yonetoku D. et al., 2004, ApJ, 609, 935

Zhao Z.-W., Wang L.-F., Zhang J.-G. et al., 2023, JCAP, 04, 022

Zheng J., Chen Y., Xu T., Zhu Z. H., 2022, Eur. Phys. J. Plus, 137, 4

Zimdahl W., Pavón D., Chimento L. P., 2001, Phys. Lett. B, 521, 133